Published in final edited form as:

Pain. 2020 March ; 161(3): 532–544. doi:10.1097/j.pain.0000000000001738.

Wnt signaling contributes to withdrawal symptoms from opioid receptor activation induced by morphine exposure or chronic inflammation

Mingzheng Wu[#a,b,c], **Zehua Li**[#a,b], **Lei Liang**[b], **Pingchuan Ma**[a], **Dong Cui**[b], **Peng Chen**[a], **Genhao Wu**[a], **Xue-Jun Song**[a,b,*]

[a]SUSTech Center for Pain Medicine and School of Medicine, Southern University of Science and Technology, Shenzhen, China

[b]Key Laboratory of Carcinogenesis and Translational Research (Ministry of Education of China), Peking University Cancer Hospital and Institute, Beijing, China

[c]Department of Neurobiology, Northwestern University, Evanston, IL, United States

[#] These authors contributed equally to this work.

Abstract

Preventing and treating opioid dependence and withdrawal is a major clinical challenge, and the underlying mechanisms of opioid dependence and withdrawal remain elusive. We hypothesized that prolonged morphine exposure or chronic inflammation-induced μ-opioid receptor activity serves as a severe stress that elicits neuronal alterations and recapitulates events during development. Here, we report that Wnt signaling, which is important in developmental processes of the nervous system, plays a critical role in withdrawal symptoms from opioid receptor activation in mice. Repeated exposures of morphine or peripheral inflammation produced by intraplantar injection of complete Freund's adjuvant significantly increase the expression of Wnt5b in the primary sensory neurons in dorsal root ganglion (DRG). Accumulated Wnt5b in DRG neurons quickly transmits to the spinal cord dorsal horn (DH) after naloxone treatment. In the DH, Wnt5b, acts through the atypical Wnt-Ryk receptor and alternative Wnt-YAP/TAZ signaling pathways, contributing to the naloxone-precipitated opioid withdrawal-like behavioral symptoms and hyperalgesia. Inhibition of Wnt synthesis and blockage of Wnt signaling pathways greatly suppress the behavioral and neurochemical alterations after naloxone-precipitated withdrawal. These findings reveal a critical mechanism underlying naloxone-precipitated opioid withdrawal, suggesting that targeting Wnt5b synthesis in DRG neurons and Wnt signaling in DH

[*]Corresponding author. Address: 1088 Xueyuan Ave, Nanshan District, Shenzhen, Guangdong 518055, China. songxuejun@sustech.edu.cn (X.-J. Song).

Conflict of interest statement

The authors have no conflicts of interest to declare.

Sponsorships or competing interests that may be relevant to content are disclosed at the end of this article.

Supplemental digital content is available for this article. Direct URL citations appear in the printed text and are provided in the HTML and PDF versions of this article on the journal's Web site (www.painjournalonline.com).

Appendix A. Supplemental digital content

Supplemental digital content associated with this article can be found online at http://links.lww.com/PAIN/A900.

may be an effective approach for prevention and treatment of opioid withdrawal syndromes, as well as the transition from acute to chronic pain.

Keywords

Wnt signaling; Morphine withdrawal; μ-opioid receptor; YAP/TAZ; Ryk receptor

1. Introduction

Wnts, a family of secreted lipid-modified signaling proteins, act as short- or long-range signaling molecules in the regulation of cellular processes, such as proliferation, differentiation, and migration during the development of nervous systems.[11,13] Typical Wnt signaling pathways include the canonical β-catenin–dependent and noncanonical β-catenin–independent pathways.[10,11,15,40,44] The core of the canonical Wnt signaling pathway is the regulation of β-catenin, a multifunctional protein that interacts with transcription factors to activate target gene transcription. The noncanonical Wnt pathways include the release of intracellular calcium and subsequent activation of calcium-calmodulin–dependent kinase[15,44] as well as the atypical Ryk-mediated pathways.[13,20,39] Transcriptional regulators YAP and TAZ are found to be key downstream effectors of the alternative Wnt signaling pathway, as they mediate the effects of Wnt ligands and regulate canonical Wnt/β-catenin signaling.[1,34,35] Ligands and receptors of Wnt signaling play critical roles in the development of the nervous system,[11,30] and regulate neuronal and synaptic plasticity in adulthood.[4,10] Dysregulation of Wnt signaling is an etiology for poor postinjury axon regeneration, certain mental disorders,[29,42] and neuropathic pain.[49] Recently, many compounds that target Wnt pathways are under clinical trials, suggesting the promise of Wnt signaling modulators in clinical practice, although some common adverse drug reactions have been indicated.[46]

Opioids are used and abused for their analgesic and euphoric effects. Repeated uses of opioids such as morphine for relief of chronic pain lead to opiate tolerance and dependence. Also, tissue inflammation and nerve injury induce μ-opioid receptor (MOR) constitutive activity, which causes latent sensitization in the dorsal horn (DH) of the spinal cord that can be unmasked by MOR antagonism.[12] Mechanisms of opiate dependence are complex and involve factors at multiple levels, including drug receptors, neuronal properties, and remodeling of brain circuits. Roles of diverse neurotransmitter systems and intracellular signaling proteins in acute and chronic opioid actions have been demonstrated.[2,6,16,19,27,31] However, despite decades of investigation, the specific cellular and molecular mechanisms underlying opioid actions remain elusive. Opiate tolerance, dependence, and the other side effects that accompany repeated administration have limited opioid use in clinical practices. Here, we report roles of Wnt signaling in opioid physical dependence and withdrawal using a well-characterized mouse model of repeated morphine usage[16] and a model of MOR constitutive activity induced by complete Freund's adjuvant (CFA) injection-induced chronic inflammation.[12] Our results show that Wnt5b is produced and accumulated in the dorsal root ganglia (DRGs) after repeated morphine treatment. Following naloxone-precipitated withdrawal, the accumulated Wnt5b in DRG can be released to the DH and activates both

the atypical noncanonical Wnt-Ryk and alternative Wnt-YAP/TAZ signaling pathways. Inhibition of Wnt5b synthesis or downstream Wnt signaling largely suppresses withdrawal behaviors, suggesting a role for the Wnt signal pathways in opioid withdrawal and the latent sensitization induced by opioid receptor activation. These findings provide potential targets in Wnt signaling for the prevention and treatment of opioid withdrawal syndromes, as well as preventing the transition from acute to chronic pain.

2. Materials

2.1. Animals, drugs, and drug administration

We purchased adult, male CD-1 mice (22–26 g-wt) from the Experimental Animal Center, Southern University of Science and Technology (SUSTech). Animals were housed at the SUSTech Animal Center in groups of 6 mice per cage under a normal 12-hour light:12-hour dark schedule, with free access to food and water. All animals were used in accordance with the regulations of the ethics committee of the International Association for the Study of Pain, and all protocols approved by the Institutional Animal Care and Use Committees. We purchased IWR-1 (Cat. 681669) and IWP-2 (681671) from EMD Millipore (Hayward, CA); Recombinant mouse Frizzled-8 Fc chimera protein (Fz-8/Fc, 112-FZ), recombinant mouse Wnt-5b protein (Wnt5b, 3006-WN), and control IgG (6–001-A) were purchased from R&D Systems (Minneapolis, MN); PEG400 and DMSO were purchased from Sigma-Aldrich St. Louis, MO and used for vehicle controls. We synthesized dCTB as we have recently described. Drug doses were selected based on previous reports and our preliminary experiments. The drugs and vehicle controls were injected intrathecally (in a total volume of 5 μL for mice) by means of lumbar puncture at the intervertebral space of L4–5 under transient anesthesia with isoflurane (1% for mice). Multiple injections through L4–5 and L5-S1 were only performed for IWP-2.

2.2. Morphine withdrawal

Mice were repeatedly injected with morphine in 7 escalating doses every 8 hours (20, 40, 60, 80, 100, 100, and 100 mg/kg, intraperitoneally). In the chronic paradigm, fixed doses of morphine (50 mg/kg/day) were injected for 10 consecutive days. Two hours after the last morphine injection, those mice received naloxone injection (1 mg/kg, subcutaneously) and the withdrawal symptoms were monitored for 30 minutes immediately after naloxone administration.[16,28] For testing the morphine withdrawal-like behavioral signs following intrathecal Wnt5b delivery, the withdrawal symptoms were monitored for 30 minutes, 8 hours after last morphine administration, without additional naloxone treatment. For naloxone-induced withdrawal symptoms in the CFA model, the withdrawal symptoms were monitored for 30 minutes immediately after naloxone administration (1 mg/kg, subcutaneously). In addition to measuring individual withdrawal signs, an overall opiate withdrawal score was calculated as: (no. of backward walking steps × 0.1) + (diarrhea × 2) + (no. of jumps × 0.1) + (paw tremor × 0.1) + no. of ptosis × 1 + no. of tremor × 1 + (% weight loss × 5) + no. of wet-dog shakes.[16,27,28] We obtained the diarrhea data by counting the frequency of watery stools from each mouse during the 30 minutes. No. of ptosis events was evaluated every 5 minutes and measured as the number of times ptosis events occurred during the evaluation period. If more than 1 ptosis occurred within a 5-minute evaluation

period, we counted it as a single event for that period. The overall withdrawal score is an arbitrary number that reflects the severity of withdrawal syndrome in the subjects, and the relative weight is determined by the frequency of each withdrawal-like behavior in the original report.[16] The relative weights are justified to ensure even contributions from individual subtotal score for each behavior.[47] Eight to 12 animals were included in each experimental group as indicated in scatter plots and figure legends. After naloxone administration, animals were individually placed in the container for behavioral assessments, with randomized number assigned to each container. Experimenters who performed behavioral tests were always blinded to treatment conditions during the assessments of withdrawal symptoms. The experimenters who performed drug administration and randomization were not involved in the behavioral assessments. All the behaviors were tested during the active phase of the animals, and the time points of morphine treatments were adjusted accordingly.

2.3. Complete freund's adjuvant model of inflammatory pain

Following baseline assessment of mechanical thresholds, the tested mouse received injection of CFA (5 μL, nondiluted) into the intraplantar surface of the left hindpaw. Sham injuries consisted of a saline injection (5 μL, 0.9%), which controlled for needle puncture and subcutaneous injection.

2.4. Assessment of mechanical allodynia

For naloxone-induced allodynia in the CFA model, the mechanical pain thresholds were measured at different time points after naloxone administration (1 mg/kg, subcutaneously). Mechanical allodynia was determined by measuring the threshold of foot withdrawal in response to mechanical stimulus of each hindpaw using a sharp, cylindrical probe with a uniform tip diameter of 0.2 mm from an Electro von Frey (ALMEMO 2390–5 Anesthesiometer; IITC Life Science, Woodland Hills, CA). The probe was applied to 6 designated loci distributed over the plantar surface of the foot. The minimal force (in grams) that induced paw withdrawal was read off of the display. Threshold of mechanical withdrawal in each animal was calculated by averaging the 6 readings, and the force was converted into milli-Newtons (mN). The results represent the mean values of ipsilateral feet. Experimenters who performed behavioral von Frey tests were always blinded to the treatment conditions.

2.5. Quantitative real-time polymerase chain reaction RT-PCR

Under deep anesthesia, the spinal cord segments of rats were quickly removed and analyzed. Total RNA was isolated with TRIzol reagent (Ambion, Austin, TX) according to the manufacturer's instructions. cDNA was then synthesized using the Takara PrimeScript Master Mix (Perfect Real Time) kit. Quantitative real-time polymerase chain reaction was performed with the DyNAmo Flash SYBR Green qPCR Kit (Thermo Fisher Scientific, Waltham, MA). The standard conditions were as follows: 95˚C for 7 minutes, then 40 cycles at 95˚C for 10 seconds and 60˚C for 30 seconds, then 95˚C for 15 seconds, 60˚C for 60 seconds, and 95˚C for 15 seconds for melt curve. Primers used for expression analysis of *wnt3a* and *wnt5b* were as follows: gene *wnt3a*: forward (5–3)-GGTGGTAGAGAAACACCGAGA; reverse (5–3)-CAGCTGACATAACAGCACCAG; gene

wnt5b: forward (5–3)-GCAAGCTGGAACTGACCAAC; reverse (5–3)-GTCCACGATCTCGGTGCATT; and gene *gapdh*: forward (5–3)-AGAGAGAGGCCCTCAGTTGCT; and reverse (5–3)-TTGTGAGGGAGATGCTCAGTGT. Relative mRNA levels were calculated using the 2-CT method. Gene expression was first normalized to the housekeeping control gene *gapdh*, and subsequently, the relative expression of genes of interest was compared with the respective experimental control.

2.6. Protein determinations

To quantify temporal changes in protein levels, Western blotting analysis was used. The spinal cord segments and DRGs (L4 and L5) were quickly removed from deeply anesthetized mice and stored at −80˚C. Sequential precipitation procedures were used on the tissue samples that were lysed in ice-cold (4˚C) NP-40 lysis buffer containing a mixture of protease inhibitor, phosphatase inhibitors, and phenylmethylsulfonyl fluoride (Sigma-Aldrich). For the analyses of nuclear YAP, TAZ, and active β-catenin, nuclear extractions were prepared using a NE-PER Nuclear and Cytoplasmic Extraction Kit (Pierce Biotechnology, Waltham, MA) according to the manufacturer's instructions. The protein concentrations of the lysates were estimated using the method of bicinchoninic acid assay (with reagents from Pierce), and the total protein content between samples was equalized. The total protein was separated by SDS-PAGE and transferred to polyvinylidene fluoride membrane (both from Bio-Rad Laboratories, Hercules, CA). The following primary antibodies were used: anti-Wnt3a (1:1000, Millipore Cat# 09–162, RRID:AB_1587634), anti-Wnt5b (1:1000, Abcam Cat# ab94914, RRID:AB_ 10675241), anti-YAP1 (1:1000; Cell Signaling Technology Cat# 4912, RRID:AB_2218911), anti-TAZ (1:1000; Cell Signaling Technology Cat# 4883, RRID:AB_1904158), anti-active β-catenin (1:1000; (Millipore Cat# 05–665, RRID:AB_309887), anti-Ryk (1:1000, Thermo Fisher Scientific Cat# PA1–30319, RRID: AB_2183043), anti-pCaMKII (Thr^{286}) (1:1000, Cell Signaling Technology Cat# 3361, RRID:AB_10015209), anti-pCREB (Ser^{133}) (1: 1000, Cell Signaling Technology Cat# 9190, RRID:AB_330498), anti-pNR1 (Ser^{897}) (1:1000; Millipore Cat# ABN99, RRID: AB_10807298), anti-pNR2B (Tyr^{1472}, 1:1000; Millipore Cat# 454583–100UL, RRID:AB_212176), anti-lamin-B (1:10000; Abcam Cat# ab133741, RRID:AB_2616597), anti-β-actin (1:2000, Bioworld Technology), and anti-GAPDH (1:8000, Sigma-Aldrich Cat# G9545, RRID:AB_796208). The membranes were then developed by enhanced chemiluminescence reagents (PerkinElmer, Waltham, MA) with horseradish peroxidase–conjugated secondary antibodies (R&D Systems, Minneapolis, MN). We used ImageJ to quantify the absolute gray-level of each blot with background subtraction, and then normalize the ratio to the control blot in each replicate. After the determination of each target protein, we incubate the same membrane with the antibodies of β-actin (total protein) or lamin-B (nuclear protein) to determine the total protein loaded. We here show them in separate images for display purpose to avoid the overexposure of the loading controls. The specificity of antibodies has been demonstrated in recent studies from our laboratory and others, in addition to that described by the vendors.[21,22,24,25,38,48]

2.7. Immunohistochemistry

Deeply anesthetized mice were perfused transcardiacally with 0.9% saline followed by 4% paraformaldehyde. The spinal cord segments and DRGs were removed and postfixed in 4%

paraformaldehyde 24 to 48 hours. After being postfixed, antigen retrieval was conducted in citric acid buffer. Then the tissues were transferred into 40% sucrose (in 0.1 M PB) for 3 days for dehydration. The tissues were sectioned at 30-μm thickness for spinal cord and DRG sections. For immunofluorescence staining, free-floating sections were blocked in phosphate buffered saline containing 10% donkey serum with 0.3% Triton X-100 for 2 hours and incubated in primary antibody at 4˚C overnight. Sections were then washed in 0.1 M phosphate buffered saline with 0.05% Triton X-100, pH 7.6 (3 × 5 minutes) followed by incubating in the secondary antibody at room temperature for 2 hours and washing. Sections were mounted on slides and covered with 90% glycerin for observation under a confocal microscope (FluoView FV1000, Olympus, Japan). The antibodies used included anti-Wnt5b (1:100, Abcam Cat# ab66616, RRID:AB_2241623), anti-c-FOS (1:1000, Synaptic Systems Cat# 226 003, RRID:AB_2231974), anti-NeuN (1:400, Millipore Cat# MAB377, RRID:AB_2298772), anti-GFAP (glial fibrillary acidic protein 1:200, Millipore Cat# IF03L-100UG, RRID:AB_10681761), anti-IBA1 (1:200, Abcam Cat# ab5076, RRID:AB_2224402), FITC conjugated isolectin B4 (IB4, 1:100, Sigma-Aldrich Cat# L2140, RRID:AB_2313663), anti-calcitonin gene-related peptide (1:100, Abcam Cat# ab139264, RRID:AB_2341090), anti-NF200 (1:100, Abcam Cat# ab40796, RRID:AB_2149620), and anti-MAP2 (1: 5000, Abcam Cat# ab75713, RRID:AB_1310432). For nucleus counterstaining, sections were incubated with 4’, 6-diamidino-2-phenylindole (DAPI 1:3000, Sigma-Aldrich) for 3 minutes at room temperature. Data were analyzed with ImageJ. To quantitatively measure the mean intensity of Wnt5b and Ryk immunofluorescence in the DH or DRGs, 3 to 5 sections from each animal were evaluated and photographed at the same exposure time to generate the raw data. The average fluorescence intensity of each pixel was normalized to the background intensity in the same image. To measure the ratio of colocalization in the DH, the percentages of overlapped pixels ($Wnt5b^+/marker^+$) from total $marker^+$ pixels were used to represent the degree of colocalization. The values from the entire DH (Under ×200 magnification) were obtained to calculate the mean intensity (pixel). To measure the Ryk internalization in the DH, the number of neurons with Ryk/DAPI overlapping was counted.

2.8. Primary culture of the dorsal horn neurons

The protocol was modified from what was previously used for DH neuron culture. Briefly, the dorsal part of the spinal cord from adult rats was dissected, minced, and then the fragments were transferred into the buffered solution containing collagenase (type IA, 1 mg/mL, Sigma) and trypsin (0.5 mg/mL). After an incubation for 30 minutes at 37˚C, the fragments were removed, rinsed, and then put into the buffered solution containing DNase (0.2 mg/mL, Sigma). Individual neurons were dissociated by passing the fragments through a set of fire-polished glass pipettes with decreasing diameter. After brief centrifugation, neurons were transferred into 10% fetal bovine serum DMEM (Dulbecco’s Modified Eagle Medium) medium in poly-D-lysine precoated confocal dishes for 3 hours followed by 72 hours incubation in neurobasal medium for primary culture. The purity of the cultured neurons was verified by immunostaining of MAP2 and DAPI staining. The cultured DH neurons of the spinal cord were visualized as round-shaped neuron bodies with processes. Most of the cells (percentage not quantified) showed MAP2-positive staining.

2.9. Calcium imaging

Primary cultured DH neurons were incubated in Fura-2/AM (5 μM) and Pluronic F-127 (0.5 mg/mL) (Thermo Fisher Scientific, Invitrogen Inc., Waltham, MA) diluted in Ringer's solution (pH = 7.4) containing 135 mM NaCl, 2 mM CaCl2, 5.4 mM KCl, 5 mM HEPES, and 5.5 mM glucose for 30 minutes. After washing, neuron fluorescence emission was measured at 520 nm following excitation at 340 nm and 380 nm (Olympus IX51 with ORCA-R2 digital camera, Hamamatsu Inc, Japan). The 340/380 nm emission ratio was used to determine intracellular calcium ($[Ca^{2+}]_i$). After loaded with Fura-2, cells with round-shaped cell bodies and multiple processes were identified as neurons and selected for imaging and quantification of calcium concentrations. At the end of all the experiments, 5 μL 10% KCl was added to bath solution to check the viability of the cells. Only those cells responded to KCl were accepted for quantification.

2.10. Statistics

Prism (GraphPad) was used to conduct all statistical analyses. All statistics were performed based on the number of animals. Alterations of detected mRNA and protein expression and the behavioral results were tested over time among groups were tested with one-way or two-way analysis of variance (ANOVA). Bonferroni's multiple comparisons were used to test specific hypotheses about differences between each operated or drug-treated group and its corresponding control group between the naive or sham animals and the treatment for Western blot or behavior data. All data are presented as mean ± SEM. The criterion for statistical significance was $P < 0.05$.

3. Results

3.1. Naloxone-precipitated morphine withdrawal induces robust increase of Wnt5b in the dorsal horn originating from the primary afferent terminals

To verify the hypothesis that Wnt signaling in the spinal cord may play a role in morphine dependence and naloxone-precipitated withdrawal, we first examined expression of Wnt family mRNA in the spinal cord using RT-PCR. Among the 19 Wnt ligands currently known, Wnt3a and Wnt5b showed elevated expression in mRNA. Wnt3a mRNA increased significantly after morphine treatment and plateaued after the naloxone-precipitated withdrawal. Wnt5b mRNA did not respond to 7 escalating doses of morphine treatment, but increased significantly following naloxone administration (Fig. 1A). In addition, expression of the mRNA levels of Wnt1, Wnt2, Wnt5a, Wnt7a, Wnt8b, Wnt9b, Wnt10b, and Wnt16 decreased after morphine treatment and naloxone-precipitated withdrawal (Fig. S1A, available as supplemental digital content at http://links.lww.com/PAIN/A900). The DRG and spinal cord tissues were taken 2 hours after the seventh dose of the escalating morphine treatment or after naloxone administration as indicated in the figures. We further examined the protein expression of Wnt3a and Wnt5b under the same conditions by western blotting. Surprisingly, Wnt3a protein expression was not altered after morphine treatment or naloxone withdrawal. By contrast, Wnt5b protein expression was rapidly and substantially increased 30 minutes after naloxone administration, and the increased expression lasted for at least 2 hours (Fig. 1B). Using immunohistochemistry, we then determined the distribution of Wnt5b in the DH after morphine withdrawal, compared with the distribution in both naïve animals

and those who received morphine treatment alone. In naïve and the morphine-treated mice, the expression of Wnt5b was sparsely distributed within the DH. However, after naloxone-precipitated withdrawal, Wnt5b was densely accumulated in the laminae I-IV (Fig. 1C). Immunoreactivity of the increased Wnt5b was predominantly localized within the afferent terminals, including the small, peptidergic fibers (CGRP-positive), and the large fibers (NF200), with some also seen in the small, nonpeptidergic fibers (IB4-positive) (Fig. 1D). Wnt5b was also heavily localized within neural soma (NeuN), local neural dendrites (MAP2), which may form the largest number of synapses with the primary afferent terminals,[8,17] and astrocytes (GFAP); however, colocalization with microglia (IBA1) reactivity was negligible (Fig. S1B, available as supplemental digital content at http://links.lww.com/PAIN/A900). Morphine treatments increased CGRP and GFAP expression in DH, while the expression of other markers was not altered (Fig. S1C, available as supplemental digital content at http://links.lww.com/PAIN/A900). These results demonstrate that naloxone-precipitated morphine withdrawal, but not morphine treatment alone, can induce a quick and significant increase of Wnt5b in the superficial layers of the DH, particularly in the primary afferent terminals.

To further examine the possibility that the increased Wnt5b in the DH may originate mainly from the primary sensory neurons, we examined the expression and distribution of Wnt5b in DRG neurons in naïve, morphine-treated, and naloxone-precipitated withdrawal animals. Western blot analysis showed that morphine treatment induced a significant increase of Wnt5b expression in the DRG, which then decreased significantly within 30 minutes and went back to baseline level within 2 hours after naloxone-precipitated withdrawal. Again, Wnt3a expression in the DRG was not changed (Fig. 1E). These results suggest that Wnt5b in the DRG is one of the sources of Wnt5b in the DH. Immunohistochemistry further showed that the immunoreactive intensity of Wnt5b was low in the naïve DRG, and its distribution was evenly across both the large-sized (NF200-positive) and small-sized CGRP-positive and IB4-positive neurons. After prolonged morphine exposure, Wnt5b expression increased significantly in the large- and medium-sized as well as the small DRG neurons. Wnt5b-positive neuronal expression was increased in NF200-positive, CGRP-positive, and IB4-positive neurons about ×4, ×2.5, and ×1.5 compared with the controls, respectively. After naloxone treatment, morphine treatment-induced Wnt5b expression was significantly decreased in the DRG neurons. In NF200-positive neurons, Wnt5b started decreasing within 30 minutes after naloxone treatment and maintained a high level for at least 2 hours. In CGRP-positive neurons, Wnt5b started decreasing within 30 minutes and returned to baseline at 2 hours after naloxone. In IB4-positive neurons, Wnt5b returned quickly back to baseline within 30 minutes after naloxone treatment. Representative immunoreactivity and data summary are shown in Fig. 1F and G. This timing of Wnt5b in DRG corresponded with the increase of Wnt5b in the DH (Fig. 1B–D).

Taken together, our results indicate that the morphine treatment induces Wnt5b accumulation mainly in DRG, and that, after morphine withdrawal, the accumulated Wnt5b is exported to the central terminals in the DH, where it may contribute to the subsequent behavioral and neurochemical alterations of morphine withdrawal.

3.2. Blocking Wnt signaling in spinal cord suppresses behavioral and neurochemical signs of naloxone-precipitated morphine withdrawal, while spinal administration of exogenous Wnt5b enhances spontaneous withdrawal behaviors

To investigate roles of spinal Wnt5b release in the action of morphine withdrawal, we examined the effects of Wnt scavenger Fz-8/Fc, a recombinant protein that mainly disrupts Wnt ligand-receptor interaction, on the behavioral and neurochemical alterations after naloxone-precipitated morphine withdrawal in mice. Intrathecal administration of Fz-8/Fc (2 μg in 5 μL saline, 30 minutes before naloxone injection) significantly suppressed both behavioral and neurochemical signs after naloxone-precipitated withdrawal, compared with IgG control (2 μg in 5 μL saline). The overall score of behavioral symptoms and individual behavioral signs (except for diarrhea and ptosis) was significantly reduced (Fig. 2A). Morphine withdrawal-induced induction of c-FOS expression, which is an indicator of increased neural excitability,[5] was greatly inhibited by Fz-8/Fc treatment in the same protocol (Fig. 2B).

In addition to blocking Wnt signaling acutely after naloxone-precipitated withdrawal, we tested whether inhibition of Wnt synthesis during morphine exposure could prevent or ameliorate the withdrawal symptoms. To address this question, IWP-2, a porcupine inhibitor that inhibits the synthesis of Wnt ligands,[9] was intrathecally injected after each dose of morphine, and its effects on the behavioral signs were observed and recorded. IWP-2 treatments at different doses (5 μg, 2 μg, and 1 μg, in 5-μL DMSO) produced significant dose-dependent suppression on naloxone-induced individual withdrawal behaviors and the overall withdrawal score (Fig. 2C). These results demonstrated that Wnt signaling activation in the spinal cord and Wnt synthesis are required in morphine withdrawal-induced neural excitability and behavioral alterations.

We then examined whether exogenous Wnt5b would be sufficient to enhance morphine withdrawal-like behaviors in naïve and morphine exposure animals. In naïve mice, intrathecal administration of a single dose of recombinant mouse Wnt5b (100 ng in 5-μL saline) did not induce gross behavioral changes. However, in animals that had received prolonged morphine treatment, a single dose of recombinant mouse Wnt5b (100 ng/5 μL) enhanced morphine withdrawal-like behaviors when animals were in the transition period to spontaneous withdrawal, 8 hours after the last morphine treatment. The overall score and 5 of 8 individual behavioral signs increased significantly (Fig. 3A). These results indicate that Wnt signaling activation is sufficient to enhance morphine withdrawal-like behavioral signs in animals with prolonged morphine exposure.

3.3. Activation of Ryk receptor contributes to behavioral and neurochemical alterations after naloxone-precipitated withdrawal

Ryk is a single-span transmembrane receptor with an intracellular tyrosine domain and a recently discovered atypical receptor involved in Wnt signaling. The Ryk receptor is required for various Wnt signaling functions involved in diverse roles in the nervous system[18,20,30,39] (Fig. 4A). After binding with Wnt5b, the Ryk receptor is cleaved by γ-secretase to release the Ryk intracellular domain, which is then translocated to the nucleus to regulate transcriptional activities.[13] We first examined the expression of Ryk receptors in the

spinal cord after morphine exposure and naloxone-precipitated withdrawal. The results showed that the prolonged exposure of morphine induced a significant increase in the full-length domain of Ryk receptors (Ryk-FL), indicating the upregulation of Ryk expression and translation. The Ryk intracellular domain (Ryk-ICD), which is the active form of Ryk receptor, showed no change after morphine exposure. However, after naloxone-precipitated withdrawal, the Ryk-ICD expression was significantly increased for at least 2 hours after naloxone injection (Fig. 4B). This increased expression of Ryk was distributed in the DH and Ryk immunoreactivity was mostly localized within neural soma and dendrites, and with astrocytes (Fig. 4C). Naloxone-precipitated withdrawal also induced intracellular accumulation of Ryk immunoreactivity. The percentage of Ryk-NeuN and Ryk-DAPI colocalization was significantly increased after naloxone treatment, compared with morphine exposure alone (Fig. 4D). These results indicate that expression and activation of Ryk receptor is correlated with prolonged morphine exposure and naloxone-precipitated withdrawal, suggesting that Ryk activation is involved in regulation of naloxone withdrawal-induced neural and behavioral alterations.

Our results further show that intrathecal administration of anti-Ryk, an antibody of Ryk (2 μg in 5 μL, given 30 minutes before naloxone), which blocks the functional activation of Ryk receptors, greatly reduced the overall score and individual behavioral signs of naloxone-precipitated morphine withdrawal (Fig. 4E). We also used calcium imaging to study the effect of Ryk receptor activation on the excitability of nociceptive secondary sensory neurons in the DH. Application of recombined Wnt5b ligands produced a significant increase of Ca^{2+} influx in the morphine-exposed animals, but not in naïve control neurons. Wnt5b-induced increase of Ca^{2+} influx and the ratio of responsive cells were greatly reduced by pretreatment with anti-Ryk (4 μg/mL in bath) (Fig. 4F). Furthermore, pretreatment with anti-Ryk significantly inhibited naloxone-precipitated withdrawal-induced phosphorylation of N-methyl-D-aspartate receptor (NMDAR) subtypes NR1 and NR2B as well as the subsequent Ca^{2+}-dependent signals CaMKII and cAMP response element-binding protein (CREB) in the spinal cord (Fig. 4G). These results indicate that increased expression of Ryk receptor in the spinal cord is involved in the latent sensitization after morphine exposure, and that activation of Ryk signaling contributes to the neuronal hyperactivity, mediating the behavioral and neurochemical alterations after naloxone-precipitated morphine withdrawal.

3.4. Activation of the transcription factors YAP, TAZ, and β-catenin contributes to the development of naloxone-precipitated withdrawal

The transcription factors YAP and TAZ are the key downstream effectors of alternative Wnt signaling, which consists of Wnt-FZD/ROR-$G\alpha_{12/13}$-Rho-Lats1/2-YAP/TAZ pathway. YAP and TAZ also mediate the effects of Wnt ligands on cell migration and osteogenic differentiation[34] (Fig. 5A). We have recently demonstrated that the YAP/TAZ activity can precisely orchestrate pain status by flipping an “ON–OFF” switch after nerve injury or activation of certain pain initiators.[45] Here, we test our hypothesis that the YAP/TAZ might also be important in the precipitation of morphine withdrawal symptoms. We determined the transcriptional activity of YAP and TAZ by examining their nuclear protein levels in the spinal cord after treatment of morphine and the following naloxone-precipitated withdrawal.

The results showed that the nuclear expression of YAP and TAZ protein remained unchanged following prolonged morphine exposure. However, naloxone-precipitated withdrawal induced significant nuclear accumulation of YAP and TAZ. The expression patterns of YAP and TAZ expression were different, such that YAP expression increased within 30 minutes and lasted for at least 2 hours after naloxone administration, while TAZ expression increased at 2 hours, but not at 30 minutes. Meanwhile, expression of the transcriptional factor β-catenin was not altered by prolonged morphine exposure, although it was transiently and significantly increased at 30 minutes and returned to baseline at 2 hours after naloxone precipitated-withdrawal (Fig. 5B).

Furthermore, we tested whether blockage of YAP/TAZ/β-catenin activity could suppress the behavioral signs of morphine withdrawal. Intrathecal administration of dCTB (200 μg in 5 μL, given 30 minutes before naloxone injection), a reagent that inhibits nuclear activity of YAP/TAZ/β-catenin through GSK-3 and MST/LATS,[45] greatly suppressed the overall score and individual behavioral signs of naloxone-precipitated withdrawal. To selectively inhibit β-catenin, we used IWR-1, an Axin activator that inhibits nuclear translocation of β-catenin. IWR-1 (5 μg in 5 μL, 30 minutes before naloxone injection) also produced significant suppression on the overall score and individual behavioral signs of naloxone-precipitated withdrawal (Fig. 5C). These results suggest that YAP, TAZ, and β-catenin are each involved in development of morphine withdrawal but may have different regulatory effects on the development of morphine withdrawal.

3.5. Wnt signaling contributes to withdrawal symptoms from prolonged μ-opioid receptor activity induced by chronic morphine exposure or inflammation

We continued to test our hypothesis that Wnt signaling might also be involved in chronic exposure of morphine and not just in acute morphine exposure as we described above. Chronic morphine administration at a fixed dose (50 mg/kg/day) for 10 consecutive days recapitulates a more appropriate condition in clinical practice (Fig. 6A). Naloxone administration in this paradigm induced comparable levels of withdrawal behaviors. IWP-2 treatments after each dose of morphine suppressed future withdrawal after naloxone injection in a dose-dependent manner. Furthermore, acute administration of IWR-1 before naloxone treatment also reduced the severity of withdrawal (Fig. 6B and C). These results suggest that, in addition to effects induced by acute morphine exposure, Wnt signaling also contributes to the withdrawal from prolonged MOR activity induced by chronic exposure of morphine.

Chronic inflammation or tissue injury induces MOR constitutive activity, and opioid antagonist application can restore previous tissue injury-induced pain hypersensitivity,[12,43] suggesting that the cessation of such tonic constitutive activity of MOR may play a key role in the transition from acute to chronic pain. Given that Wnt signaling is critical in withdrawal after prolonged exogenous morphine treatment, we asked whether Wnt signaling might be also involved in the MOR constitutive activity after chronic inflammation. We examined this idea using a recently described mouse model.[12] A unilateral intraplantar injection of CFA in mice produced mechanical allodynia that recovered within 2 weeks. However, when delivered 21 days after CFA injection, subcutaneous injection of naloxone (1

mg/kg) completely restored the mechanical allodynia. This result indicated a pre-existing endogenous opioid dependence (Fig. 7A and B). After naloxone injection on the 21st day after CFA, the mechanical nociceptive threshold decreased significantly starting within 30 minutes, was maintained at a constant low level for at least 90 minutes, and returned to baseline within 3 hours. Interestingly, such MOR antagonist (naloxone)-induced hyperalgesia in animals with pre-existing endogenous opioid dependence was significantly suppressed or prevented by intrathecal administration of Wnt ligand scavenger, Fz-8/Fc (2 μg in 5 μL), and Ryk receptor functional blocker, anti-Ryk (2 μg in 5 μL), 30 minutes before naloxone injection (Fig. 5B). These results indicate that Wnt signaling may also contribute to the processing of CFA-generated MOR constitutive activity and MOR antagonist-evoked painful and somatomotor symptoms.

We then examined expression of Wnt5b in animals that previously received CFA injection. The results showed that Wnt5b immunoreactivity was not altered by CFA treatment alone but was significantly increased after naloxone treatment on the 21st day after CFA injection (Fig. 7C). The increased Wnt5b expression was distributed in the superficial layers of the DH and mostly localized in the primary afferents, including the CGRP-, IB4-, and NF200-positive terminals (Fig. 7D). Furthermore, we found that on the 21st day after CFA, expression of Wnt5b was significantly increased in the DRG and then reduced after naloxone treatment (Fig. 7E). These findings strongly support the idea that the increased Wnt5b in the superficial DH in the condition of chronic peripheral inflammation also predominantly originated from its peripheral afferent terminals, the central axons of DRG neurons.

Interestingly, subcutaneous injection of MOR antagonist naloxone also precipitated somatomotor behaviors including backward walking, jumping, paw tremor, and wetdog shake on the 21st day in animals that developed MOR constitutive activity in the CFA model. These morphine withdrawal-like symptoms were prevented or significantly suppressed by pretreatment with the Wnt scavenger Fz-8/Fc and Ryk receptor blocker anti-Ryk, respectively (Fig. 7F). These findings strongly support the idea that Wnt signaling plays important roles in not only classical morphine withdrawal, but also the latent sensitization following chronic inflammation. The latter has been considered an important mechanism underlying the chronification of acute pain.[43]

4. Discussion

Our study reveals a critical role for Wnt signaling in opioid withdrawal through the Wnt-Ryk and Wnt-YAP/TAZ signaling axes. After prolonged MOR activation induced by prolonged morphine treatment or previous tissue inflammation, naloxone-precipitated withdrawal induces significant increase of Wnt5b expression in primary sensory afferents in DH. Wnt signaling may contribute to the subsequent withdrawal behaviors and neurochemical alterations through the atypical noncanonical Wnt-Ryk and the alternative Wnt-YAP/TAZ signaling pathways. We believe that these findings may support a new mechanism underlying opioid dependence and withdrawal symptoms following prolonged morphine exposure and chronic inflammation-induced opioid receptor activation. This study

also provides potential targets in Wnt-Ryk and Wnt-YAP/TAZ signaling axes for the prevention of opioid withdrawal syndromes and chronification of acute pain.

Wnts are known to be important for various developmental processes. Studies have demonstrated the dysregulation of Wnt signaling in certain diseases and disorders. For example, Wnt signaling is upregulated in schizophrenic brains[14] and peripheral nerve-injured DRG and spinal cord,[41,49] as well as downregulated in brains with Alzheimer disease.[7,32] Here, we show that prolonged morphine treatment causes expression and accumulation of Wnt5b in DRG; naloxone-precipitated withdrawal induces apparent, rapid export of Wnt5b from DRG and robust increase of Wnt5b in the superficial DH, where Wnt5b may originate predominantly from the DRG afferent terminals. Another possibility for the increased Wnt5b might be that naloxone quickly increases the synthesis of Wnt5b in the DRG soma and terminals, but also stimulates a degradation of Wnt5b that is slower in the terminals. We noticed the broad changes of Wnt5b expression in various myelinated and unmyelinated DRG and DH cells. These perhaps reflect some morphine-mediated effects in MOR^+ afferents and DH neurons, which could then indirectly influence the expression of Wnt5b in DRG neurons that may lack MOR expression. Surprisingly, the expression of another important Wnt ligand, Wnt3a, did not show any alteration in DRG and the DH, although its mRNA expression was increased after morphine and naloxone treatment.

The Wnt-Ryk signaling pathway is one of the major noncanonical, β-catenin–independent Wnt pathways, in which the atypical Ryk receptor may mediate Wnt activation of intracellular signaling cascades.[13,18,26,36] Here, our results show that the prolonged morphine exposure induces upregulation, translation, and naloxone withdrawal-induced activation of Ryk receptor in the neuronal somata and dendrites in the DH. These changes correspond with Wnt5b alterations. Spinal blockade of Ryk receptor with the Ryk antibody suppresses morphine withdrawal-induced behavioral signs and the accompanying neurochemical alterations. Thus, these findings support the idea that the spinal Wnt-Ryk signaling axis is important in the sensitization and the hyperactivity induced by withdrawal. A potential mechanism of Wnt-Ryk signaling is the regulation of signal transduction and synaptic plasticity, which have been considered essential to the spinal central sensitization.

The transcription factors YAP and TAZ are key downstream effectors of alternative Wnt signaling, while both of them mediate the effects of WNT ligands on cell migration and osteogenic differentiation.[34] Here, we demonstrate that naloxone-precipitated morphine withdrawal induces activation of YAP and TAZ in the DH, in addition to increasing the levels of Wnt5b in the DH. Spinal blockade of YAP/TAZ activity suppresses the behavioral signs of naloxone-precipitated withdrawal. YAP/TAZ inhibition reduced NLX-precipitated withdrawal effects similarly to the Wnt scavenger FZ-8/Fc. These findings indicate that the alternative Wnt-YAP/TAZ signaling axis also participates in the withdrawal symptoms from morphine.

Constitutive activation of MOR induced by the activation of spinal pain pathways suppresses the primary pain caused by nerve inflammation or injury.[12] The complex effect of constitutive MOR activity may promote latent sensitization in the spinal DH. Unmasking of latent sensitization caused by antagonism of MOR may restore the original pain.[43] Improper

cessation of tonic constitutive activity of MOR after injury may play a key role in the transition from acute to chronic pain.[12] We have recently reported that CFA-produced tissue injury induces activation of the Wnt/FZD/β-catenin signaling pathway (onset within 24 hours and lasting for at least 72 hours).[49] Here, our results further show that, on day 21 after CFA when Wnt5b expression and the mechanical hyperalgesia had recovered to their baseline, naloxone administration reproduces the elevated Wnt5b immunoreactivity in the DH as well as the mechanical allodynia or hyperalgesia and withdrawal symptoms. Wnt5b in the superficial DH, which is transported from the DRG neurons, then activates downstream signaling and mediates withdrawal symptoms. These findings support the idea that Wnt expression and secretion may be regulated by opioid receptor activation.[3,23,33,37] The interaction between Wnt and MOR can be an important mechanism for Wnt signaling to trigger or enhance withdrawal symptoms. Furthermore, such hyperalgesia and withdrawal symptoms can be inhibited by spinal administration of Wnt scavenger Fz-8/Fc or functional blocker of Ryk receptor. These findings strongly support potential clinical interventions targeting Wnt signaling to treat opioid withdrawal and the opioid-induced sensitization. The latent sensitization induced by opioid receptor activation is considered a key event in chronification of acute pain.[43] We noticed that compound administration by intrathecal injection may also reach the DRG, in addition to the spinal cord. Thus, intrathecal injection of Wnt inhibitors may also act by disrupting the Wnt signaling pathway within the DRG-spinal cord loop to suppress withdrawal behaviors. Moreover, inhibition of Wnt signaling in the spinal cord may disrupt the feed-forward sensitization caused by primary pain and repeated opioid receptor activation.[12,43,49] These findings may suggest a new mechanism of opioid-induced sensitization and provide a potential target for the prevention of transition from acute to chronic pain.

Supplementary Material

Refer to Web version on PubMed Central for supplementary material.

Acknowledgements

The authors thank Angela A. Song at University of Pennsylvania Perelman School of Medicine for editing English throughout the manuscript. This work was partly supported by the National Natural Science Foundation of China (NFSC81320108012), Beijing Natural Science Foundation (#7191001), Science and Technology Planning Project of Guangdong Province 2018B030331001 and Southern University of Science and Technology (G02416002). Mingzheng Wu was supported as an affiliate fellow of the NIH T32 AG20506. Author contributions: X.-J. S. and M.W. designed research studies; M.W., Z.L., L.L., P.M., D.C., P.C., and G.W. conducted experiments and acquired data; M.W., and X.-J.S. analyzed data; X.-J. S and M.W. wrote the manuscript. This work should be attributed equally to the institutions “SUSTech Center for Pain Medicine and School of Medicine, Southern University of Science and Technology, Shenzhen, China” and “Key Laboratory of Carcinogenesis and Translational Research (Ministry of Education of China), Peking University Cancer Hospital and Institute, Beijing, China.”

References

[1]. Azzolin L, Panciera T, Soligo S, Enzo E, Bicciato S, Dupont S, Bresolin S, Frasson C, Basso G, Guzzardo V, Fassina A, Cordenonsi M, Piccolo S. YAP/TAZ incorporation in the beta-catenin destruction complex orchestrates the Wnt response. Cell 2014;158:157–70. [PubMed: 24976009]

[2]. Bajo M, Crawford EF, Roberto M, Madamba SG, Siggins GR. Chronic morphine treatment alters expression of N-methyl-D-aspartate receptor subunits in the extended amygdala. J Neurosci Res 2006;83:532–7. [PubMed: 16453311]

[3]. Banziger C, Soldini D, Schutt C, Zipperlen P, Hausmann G, Basler K. Wntless, a conserved membrane protein dedicated to the secretion of Wnt proteins from signaling cells. Cell 2006;125:509–22. [PubMed: 16678095]

[4]. Budnik V, Salinas PC. Wnt signaling during synaptic development and plasticity. Curr Opin Neurobiol 2011;21:151–9. [PubMed: 21239163]

[5]. Bullitt E Expression of c-fos-like protein as a marker for neuronal activity following noxious stimulation in the rat. J Comp Neurol 1990;296:517–30. [PubMed: 2113539]

[6]. Burma NE, Bonin RP, Leduc-Pessah H, Baimel C, Cairncross ZF, Mousseau M, Shankara JV, Stemkowski PL, Baimoukhametova D, Bains JS, Antle MC, Zamponi GW, Cahill CM, Borgland SL, De Koninck Y, Trang T. Blocking microglial pannexin-1 channels alleviates morphine withdrawal in rodents. Nat Med 2017;23:355–60. [PubMed: 28134928]

[7]. Caricasole A, Copani A, Caraci F, Aronica E, Rozemuller AJ, Caruso A, Storto M, Gaviraghi G, Terstappen GC, Nicoletti F. Induction of Dickkopf-1, a negative modulator of the Wnt pathway, is associated with neuronal degeneration in Alzheimer's brain. J Neurosci 2004;24:6021–7. [PubMed: 15229249]

[8]. Chao HT, Zoghbi HY, Rosenmund C. MeCP2 controls excitatory synaptic strength by regulating glutamatergic synapse number. Neuron 2007;56:58–65. [PubMed: 17920015]

[9]. Chen B, Dodge ME, Tang W, Lu J, Ma Z, Fan CW, Wei S, Hao W, Kilgore J, Williams NS, Roth MG, Amatruda JF, Chen C, Lum L. Small moleculemediated disruption of Wnt-dependent signaling in tissue regeneration and cancer. Nat Chem Biol 2009;5:100–7. [PubMed: 19125156]

[10]. Chen J, Park CS, Tang SJ. Activity-dependent synaptic Wnt release regulates hippocampal long term potentiation. J Biol Chem 2006;281:11910–16. [PubMed: 16501258]

[11]. Ciani L, Salinas PC. WNTs in the vertebrate nervous system: from patterning to neuronal connectivity. Nat Rev Neurosci 2005;6:351–62. [PubMed: 15832199]

[12]. Corder G, Doolen S, Donahue RR, Winter MK, Jutras BL, He Y, Hu X, Wieskopf JS, Mogil JS, Storm DR, Wang ZJ, McCarson KE, Taylor BK. Constitutive mu-opioid receptor activity leads to long-term endogenous analgesia and dependence. Science 2013;341:1394–9. [PubMed: 24052307]

[13]. Fradkin LG, Dura JM, Noordermeer JN. Ryks: new partners for Wnts in the developing and regenerating nervous system. Trends Neurosci 2010;33:84–92. [PubMed: 20004982]

[14]. Ftouh S, Akbar MT, Hirsch SR, de Belleroche JS. Down-regulation of Dickkopf 3, a regulator of the Wnt signalling pathway, in elderly schizophrenic subjects. J Neurochem 2005;94:520–30. [PubMed: 15998302]

[15]. Fuerer C, Nusse R, Ten Berge D. Wnt signalling in development and disease. Max delbruck center for molecular medicine meeting on Wnt signaling in development and disease. EMBO Rep 2008;9:134–8. [PubMed: 18188179]

[16]. Georgescu D, Zachariou V, Barrot M, Mieda M, Willie JT, Eisch AJ, Yanagisawa M, Nestler EJ, DiLeone RJ. Involvement of the lateral hypothalamic peptide orexin in morphine dependence and withdrawal. J Neurosci 2003;23:3106–11. [PubMed: 12716916]

[17]. Harada A, Teng J, Takei Y, Oguchi K, Hirokawa N. MAP2 is required for dendrite elongation, PKA anchoring in dendrites, and proper PKA signal transduction. J Cel Biol 2002;158:541–9.

[18]. Hollis ER II, Ishiko N, Yu T, Lu CC, Haimovich A, Tolentino K, Richman A, Tury A, Wang SH, Pessian M, Jo E, Kolodkin A, Zou Y. Ryk controls remapping of motor cortex during functional recovery after spinal cord injury. Nat Neurosci 2016;19:697–705. [PubMed: 27065364]

[19]. Inoue M, Mishina M, Ueda H. Locus-specific rescue of GluRepsilon1 NMDA receptors in mutant mice identifies the brain regions important for morphine tolerance and dependence. J Neurosci 2003;23:6529–36. [PubMed: 12878694]

[20]. Inoue T, Oz HS, Wiland D, Gharib S, Deshpande R, Hill RJ, Katz WS, Sternberg PW. C. elegans LIN-18 is a Ryk ortholog and functions in parallel to LIN-17/Frizzled in Wnt signaling. Cell 2004;118:795–806. [PubMed: 15369677]

[21]. Jia D, Yang W, Li L, Liu H, Tan Y, Ooi S, Chi L, Filion LG, Figeys D, Wang L. β-catenin and NF-κB co-activation triggered by TLR3 stimulation facilitates stem cell-like phenotypes in breast cancer. Cell Death Differ 2015;22:298. [PubMed: 25257174]

[22]. Jin H, Xue L, Mo L, Zhang D, Guo X, Xu J, Li J, Peng M, Zhao X, Zhong M, Xu D, Wu XR, Huang H, Huang C. Downregulation of miR-200c stabilizes XIAP mRNA and contributes to invasion and lung metastasis of bladder cancer. Cell Adh Migr 2019;13:236–48. [PubMed: 31240993]

[23]. Jin J, Kittanakom S, Wong V, Reyes BAS, Van Bockstaele EJ, Stagljar I, Berrettini W, Levenson R. Interaction of the mu-opioid receptor with GPR177 (Wntless) inhibits Wnt secretion: potential implications for opioid dependence. BMC Neurosci 2010;11:33. [PubMed: 20214800]

[24]. Kato S, Hayakawa Y, Sakurai H, Saiki I, Yokoyama S. Mesenchymal-transitioned cancer cells instigate the invasion of epithelial cancer cells through secretion of WNT3 and WNT5B. Cancer Sci 2014;105:281–9. [PubMed: 24344732]

[25]. Li X, Wu XQ, Deng R, Li DD, Tang J, Chen WD, Chen JH, Ji J, Jiao L, Jiang S, Yang F, Feng GK, Senthilkumar R, Yue F, Zhang HL, Wu RY, Yu Y, Xu XL, Mai J, Li ZL, Peng XD, Huang Y, Huang X, Ma NF, Tao Q, Zeng YX, Zhu XF. CaMKII-mediated Beclin 1 phosphorylation regulates autophagy that promotes degradation of Id and neuroblastoma cell differentiation. Nat Commun 2017;8:1159. [PubMed: 29079782]

[26]. Liu S, Liu YP, Huang ZJ, Zhang YK, Song AA, Ma PC, Song XJ. Wnt/Ryk signaling contributes to neuropathic pain by regulating sensory neuron excitability and spinal synaptic plasticity in rats. PAIN 2015;156:2572–84. [PubMed: 26407042]

[27]. Liu WT, Han Y, Liu YP, Song AA, Barnes B, Song XJ. Spinal matrix metalloproteinase-9 contributes to physical dependence on morphine in mice. J Neurosci 2010;30:7613–23. [PubMed: 20519536]

[28]. Liu WT, Li HC, Song XS, Huang ZJ, Song XJ. EphB receptor signaling in mouse spinal cord contributes to physical dependence on morphine. FASEB J 2009;23:90–8. [PubMed: 18772347]

[29]. Liu Y, Wang X, Lu CC, Kerman R, Steward O, Xu XM, Zou Y. Repulsive Wnt signaling inhibits axon regeneration after CNS injury. J Neurosci 2008;28:8376–82. [PubMed: 18701700]

[30]. Lu W, Yamamoto V, Ortega B, Baltimore D. Mammalian Ryk is a Wnt coreceptor required for stimulation of neurite outgrowth. Cell 2004;119:97–108. [PubMed: 15454084]

[31]. Muscoli C, Cuzzocrea S, Ndengele MM, Mollace V, Porreca F, Fabrizi F, Esposito E, Masini E, Matuschak GM, Salvemini D. Therapeutic manipulation of peroxynitrite attenuates the development of opiateinduced antinociceptive tolerance in mice. J Clin Invest 2007;117:3530–9. [PubMed: 17975673]

[32]. Nishimura M, Yu G, Levesque G, Zhang DM, Ruel L, Chen F, Milman P, Holmes E, Liang Y, Kawarai T, Jo E, Supala A, Rogaeva E, Xu DM, Janus C, Levesque L, Bi Q, Duthie M, Rozmahel R, Mattila K, Lannfelt L, Westaway D, Mount HT, Woodgett J, St George-Hyslop P. Presenilin mutations associated with Alzheimer disease cause defective intracellular trafficking of beta-catenin, a component of the presenilin protein complex. Nat Med 1999;5:164–9. [PubMed: 9930863]

[33]. Packard M, Koo ES, Gorczyca M, Sharpe J, Cumberledge S, Budnik V. The Drosophila Wnt, wingless, provides an essential signal for pre- and postsynaptic differentiation. Cell 2002;111:319–30. [PubMed: 12419243]

[34]. Park HW, Kim YC, Yu B, Moroishi T, Mo JS, Plouffe SW, Meng Z, Lin KC, Yu FX, Alexander CM, Wang CY, Guan KL. Alternative Wnt signaling activates YAP/TAZ. Cell 2015;162:780–94. [PubMed: 26276632]

[35]. Piccolo S, Dupont S, Cordenonsi M. The biology of YAP/TAZ: hippo signaling and beyond. Physiol Rev 2014;94:1287–312. [PubMed: 25287865]

[36]. Rao TP, Kuhl M. An updated overview on Wnt signaling pathways: a prelude for more. Circ Res 2010;106:1798–806. [PubMed: 20576942]

[37]. Reyes BA, Vakharia K, Ferraro TN, Levenson R, Berrettini WH, Van Bockstaele EJ. Opiate agonist-induced re-distribution of Wntless, a mu-opioid receptor interacting protein, in rat striatal neurons. Exp Neurol 2012;233:205–13. [PubMed: 22001156]

[38]. Richards MH, Seaton MS, Wallace J, Al-Harthi L. Porcupine is not required for the production of the majority of wnts from primary human astrocytes and CD8+ T cells. PLoS One 2014;9:e92159. [PubMed: 24647048]

[39]. Schmitt AM, Shi J, Wolf AM, Lu CC, King LA, Zou Y.Wnt-Ryksignalling mediates medial-lateral retinotectal topographic mapping. Nature 2006;439:31–7. [PubMed: 16280981]

[40]. Shimizu H, Julius MA, Giarre M, Zheng Z, Brown AM, Kitajewski J. Transformation by Wnt family proteins correlates with regulation of beta-catenin. Cell Growth Differ 1997;8:1349–58. [PubMed: 9419423]

[41]. Simonetti M, Agarwal N, Stosser S, Bali KK, Karaulanov E, Kamble R, Pospisilova B, Kurejova M, Birchmeier W, Niehrs C, Heppenstall P, Kuner R. Wnt-Fzd signaling sensitizes peripheral sensory neurons via distinct noncanonical pathways. Neuron 2014;83:104–21. [PubMed: 24991956]

[42]. Suh HI, Min J, Choi KH, Kim SW, Kim KS, Jeon SR. Axonal regeneration effects of Wnt3a-secreting fibroblast transplantation in spinal cord-injured rats. Acta Neurochir (Wien) 2011;153:1003–10. [PubMed: 21249402]

[43]. Taylor BK, Corder G. Endogenous analgesia, dependence, and latent pain sensitization. Curr Top Behav Neurosci 2014;20:283–325. [PubMed: 25227929]

[44]. Tu X, Joeng KS, Nakayama KI, Nakayama K, Rajagopal J, Carroll TJ, McMahon AP, Long F. Noncanonical Wnt signaling through G protein-linked PKCdelta activation promotes bone formation. Dev Cel 2007;12:113–27.

[45]. Xu N, Wu MZ, Deng XT, Ma PC, Li ZH, Liang L, Xia MF, Cui D, He DD, Zong Y, Xie Z, Song XJ. Inhibition of YAP/TAZ activity in spinal cord suppresses neuropathic pain. J Neurosci 2016;36:10128–40. [PubMed: 27683908]

[46]. Yang K, Wang X, Zhang H, Wang Z, Nan G, Li Y, Zhang F, Mohammed MK, Haydon RC, Luu HH, Bi Y, He TC. The evolving roles of canonical WNT signaling in stem cells and tumorigenesis: implications in targeted cancer therapies. Lab Invest 2016;96:116–36. [PubMed: 26618721]

[47]. Zachariou V, Brunzell DH, Hawes J, Stedman DR, Bartfai T, Steiner RA, Wynick D, Langel U, Picciotto MR. The neuropeptide galanin modulates behavioral and neurochemical signs of opiate withdrawal. Proc Natl Acad Sci U S A 2003;100:9028–33. [PubMed: 12853567]

[48]. Zhang L, Cheng F, Wei Y, Zhang L, Guo D, Wang B, Li W. Inhibition of TAZ contributes radiation-induced senescence and growth arrest in glioma cells. Oncogene 2019;38:2788–99. [PubMed: 30542117]

[49]. Zhang YK, Huang ZJ, Liu S, Liu YP, Song AA, Song XJ. WNT signaling underlies the pathogenesis of neuropathic pain in rodents. J Clin Invest 2013;123:2268–86. [PubMed: 23585476]

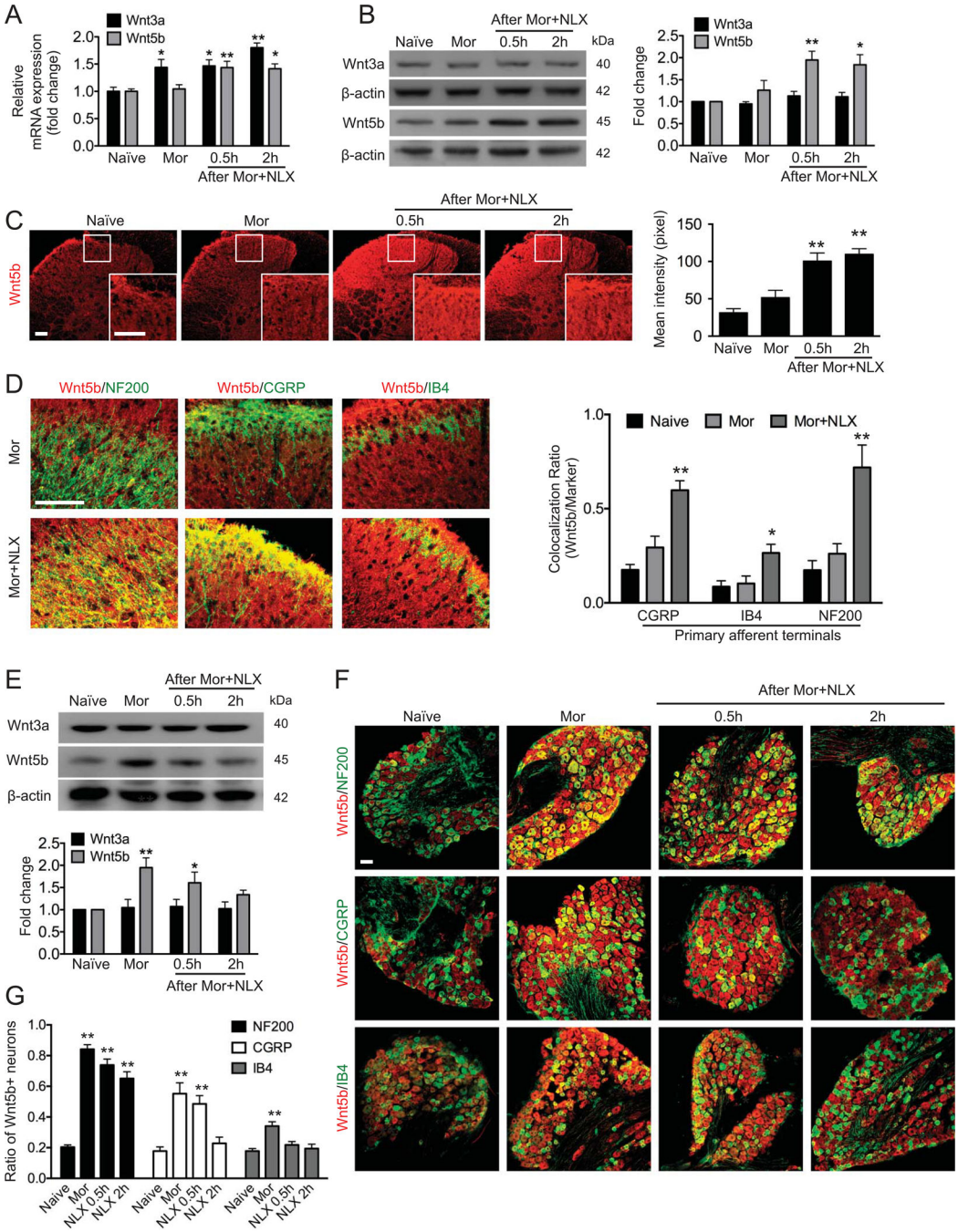

Figure 1.

Naloxone-precipitated morphine withdrawal induces a quick and significant increase of Wnt5b expression in the DH originating from DRG neurons. (A) Expression of Wnt3a and Wnt5b mRNA in the DH. Wnt3a, one-way ANOVA, $P = 0.0005$. Bonferroni's multiple comparisons vs naive: Mor, $P = 0.0392$, after NLX 0.5 hours, $P = 0.02$, 2 hours, $P = 0.0001$.Wnt5b, one-way ANOVA, $P = 0.0027$.Bonferroni'smultiple comparisons vs naive: Mor, $P > 0.99$, After NLX 0.5 hours, $P = 0.0078$, 2 hours, $P = 0.0114$. (B) Expression ofWnt3a andWnt5b protein in the DH (Wnt3a, one-way ANOVA, $P = 0.3174$. Wnt5b, one-

way ANOVA, $P = 0.0044$. Bonferroni's multiple comparisons vs naive: Mor, $P > 0.99$, After NLX 0.5 hours, $P = 0.0054$, 2 hours, $P = 0.0138$). Left, representative Western blotting bands. Right, data summary (mean ± SEM). (C) Immunofluorescence showing expression of Wnt5b (red) in the DH (left). Histogram showing the mean intensity of Wnt5b immunofluorescent activity (right) (one-way ANOVA, $P < 0.0001$. Bonferroni's multiple comparisons vs naive: Mor, $P = 0.3389$, after NLX 0.5 hours, $P < 0.0001$, 2 hours, $P = 0.0001$). Original magnifications: ×200, scale bar = 50 μm. (D) Colocalization ofWnt5b (red) with primary sensory afferents (NF200, CGRP, and IB4, green) in the DH. Left: representative immunofluorescent activity. Original magnifications: ×800, scale bar = 50 μm. Right: Colocalization ratio of Wnt5b with CGRP (one-way ANOVA, $P < 0.0001$. Bonferroni's multiple comparisons vs naive: Mor, $P = 0.2186$, After NLX, $P < 0.0001$), IB4 (One-way ANOVA, $P = 0.0141$. Bonferroni's multiple comparisons vs naive: Mor, $P > 0.99$, after NLX, $P = 0.0158$) and NF200 (one-way ANOVA, $P = 0.001$. Bonferroni's multiple comparisons vs naive: Mor, $P = 0.9307$, after NLX, $P = 0.001$) following different treatments (Right). (E) Expression of Wnt3a and Wnt5b in DRG (Wnt3a, one-way ANOVA, $P = 0.9876$. Wnt5b, one-way ANOVA, $P = 0.0037$. Bonferroni's multiple comparisons vs naive: Mor, $P = 0.0015$, after NLX 0.5 hours, $P = 0.0402$, 2 hours, $P = 0.4257$). Top: representative Western blot bands. Bottom, data summary (mean ± SEM). (F) Immunofluorescence showing expression and cellular distribution of Wnt5b in DRG neurons (marked with NF200, CGRP and IB4).Original magnifications: ×200, scale bar = 50 μm. (G) Histogram showing the ratio of Wnt5b-positive neurons in NF200 (one-way ANOVA, $P < 0.0001$. Bonferroni's multiple comparisons vs naive: Mor, $P < 0.0001$, after NLX 0.5 hours, $P < 0.0001$, 2 hours, $P < 0.0001$), CGRP (one-way ANOVA, $P < 0.0001$. Bonferroni's multiple comparisons vs naive: Mor, $P < 0.0001$, after NLX 0.5 hours, $P = 0.0006$, 2 hours, $P > 0.99$) and IB4 (one-way ANOVA, $P = 0.0002$. Bonferroni's multiple comparisons vs naive: Mor, $P = 0.0002$, after NLX 0.5 hours, $P = 0.7622$, 2 hours, $P > 0.99$) positive DRG neurons. $^{*}P < 0.05$, $^{**}P < 0.01$ vs naïve. Number of animals included in each group: 5 in A–D, 4 in E, and 8 in G. ANOVA, analysis of variance; DH, dorsal horn; Mor = morphine; NLX = naloxone.

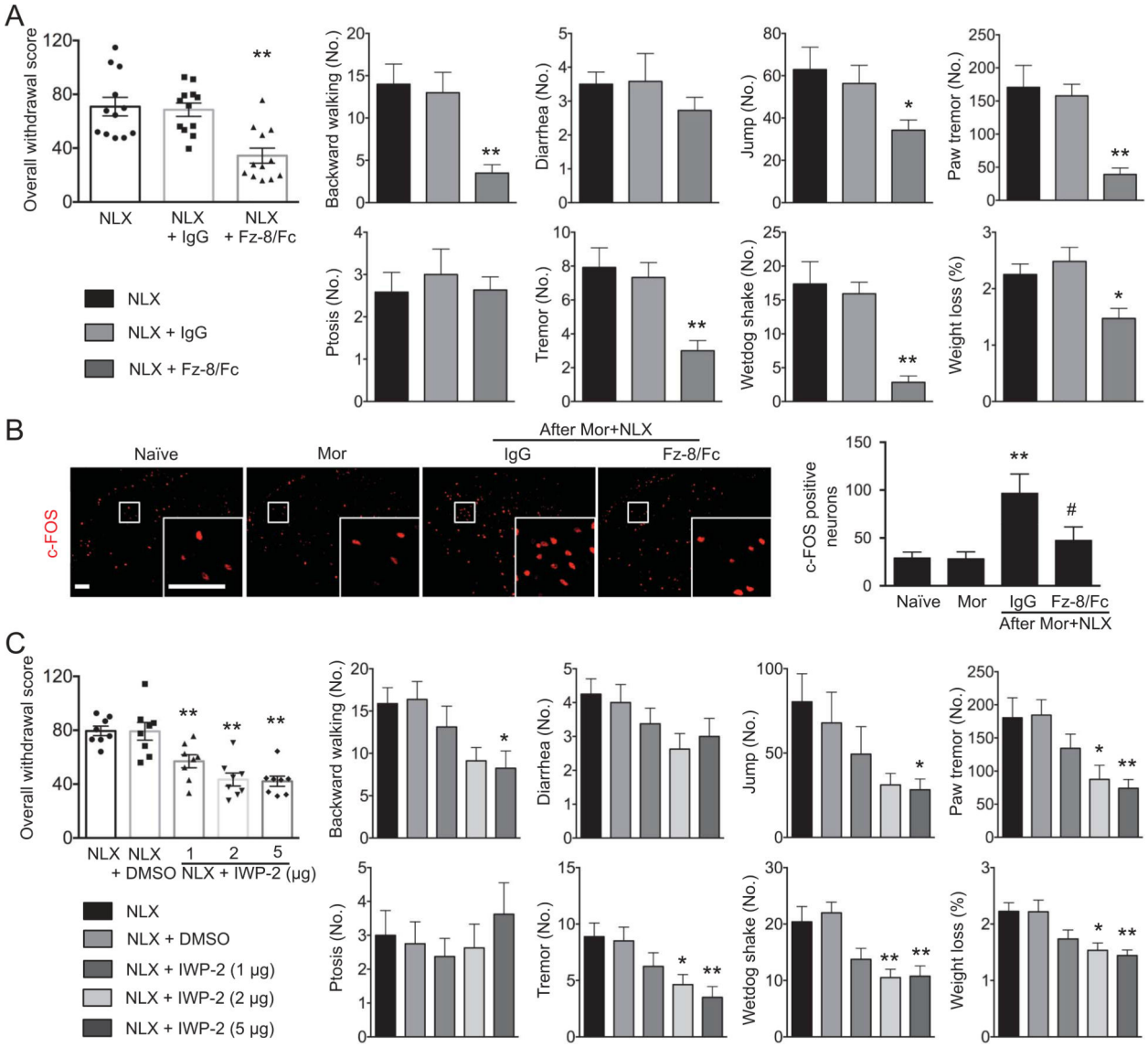

Figure 2.

Inhibition of Wnt signaling suppresses naloxone-precipitated withdrawal. (A) Intrathecal administration of Wnt scavenger Fz-8/Fc inhibited the overall withdrawal scores (left) and individual behavioral signs after withdrawal (one-way ANOVA, $P < 0.0001$. Bonferroni's multiple comparisons vs NLX: IgG, $P > 0.99$, after Fz-8/Fc, $P = 0.0002$). $*P < 0.05$, $**P < 0.01$ vs NLX. Individual signs (Bonferroni's multiple comparisons, NLX + Fz-8/Fc vs NLX, backward walking, $P = 0.0018$, diarrhea, $P = 0.7008$, jump, $P = 0.0420$, paw tremor, $P = 0.0004$, ptosis, $P > 0.99$, tremor, $P = 0.0011$, Wetdog shake, $P = 0.0001$, weight loss, $P = 0.0269$) (B) Immunofluorescence showing effects of Wnt scavenger Fz-8/Fc on induction of c-FOS in the DH. Fz-8/Fc, 2 μg in 5 μL, intrathecally 30 minutes before naloxone administration (One-way ANOVA, $P = 0.0069$. Bonferroni's multiple comparisons, after Mor + NLX, IgG vs naïve, $P = 0.0049$, Fz-8/Fc vs IgG, $P = 0.0374$). Tissues were collected 30 minutes after naloxone injection (n = 5 animals, 4 spinal cord sections from each animal in each group, edge stainings were excluded from quantification). Original magnification:

×200s, scale bar = 50 μm. **$P < 0.01$ vs naive. #$P < 0.05$ vs Mor + NLX + IgG. (C) Intrathecal administration of Wnt synthesis inhibitor IWP-2 after each morphine treatment inhibited the overall withdrawal scores (left) and individual behavioral signs after naloxone-precipitated withdrawal (one-way ANOVA, $P < 0.0001$. Bonferroni's multiple comparisons vs NLX: IWP-2, 1 μg, $P = 0.0087$, 2 μg, $P < 0.0001$, 5 μg, $P < 0.0001$). **$P < 0.01$ vs NLX. Individual signs (Bonferroni's multiple comparisons, NLX + IWP-2 (1, 2, 5 μg) vs NLX, backward walking, $P > 0.99$, $P = 0.0998$, $P = 0.0484$, diarrhea, $P = 0.8605$, $P = 0.0994$, $P = 0.3197$, jump, $P = 0.4892$, $P = 0.0665$, $P = 0.0465$, paw tremor, $P = 0.6322$, $P = 0.0248$, $P = 0.0081$, ptosis, $P > 0.99$, tremor, $P = 0.4160$, $P = 0.0422$, $P = 0.0065$,Wetdog shake, $P = 0.1030$, $P = 0.0056$, $P = 0.0071$, weight loss, $P = 0.1237$, $P = 0.0122$, $P = 0.0039$). *$P < 0.05$, **$P < 0.01$ vs NLX. Number of animals included in each group: 12, 5, and 8 in A, B, and C, respectively. ANOVA, analysis of variance; CFA, complete Freund's adjuvant; DH, dorsal horn; Mor = morphine; NLX = naloxone.

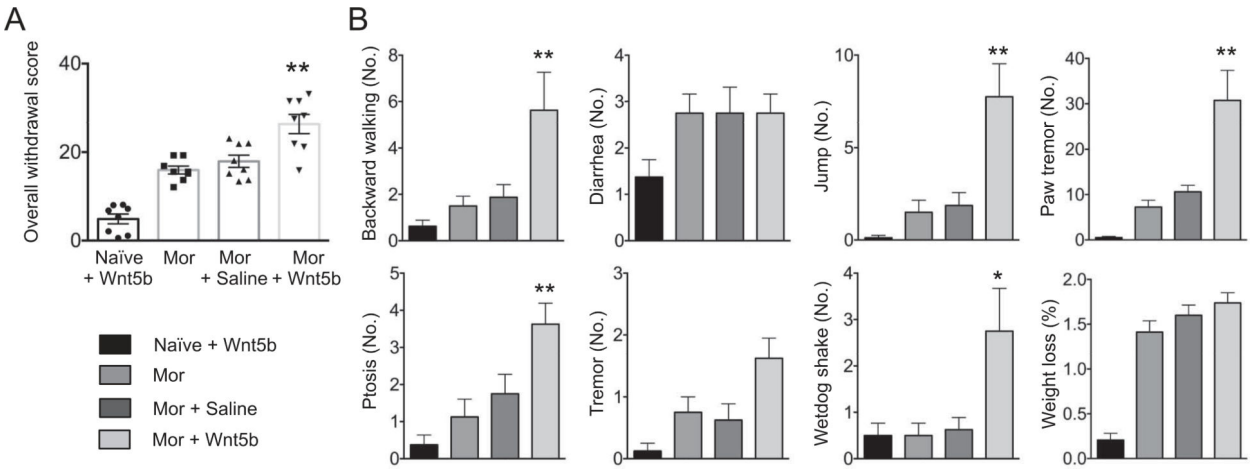

Figure 3.

Exogenous Wnt5b administration enhances spontaneous withdrawal behaviors. Intrathecal injection of Wnt5b (100 ng in 5 μL saline)-induced morphine withdrawal-like behavioral signs in animals with prolonged morphine exposure. Wnt5b or saline was injected 8 hours after last morphine treatment. Behavioral signs were recorded (30 minutes), 0.5 hours after Wnt5b injection. (A) Overall withdrawal scores. (B) Individual behavioral signs. Eight animals in each of the 4 groups. One-way ANOVA, $P < 0.0001$. Bonferroni's multiple comparisons vs Mor: After saline, $P > 0.99$, after Wnt5b, $P < 0.0001$. Individual signs (Bonferroni's multiple comparisons, Mor + Wnt5b vs Mor, backward walking, $P = 0.009$, diarrhea, $P > 0.99$, jump, $P = 0.005$, paw tremor, $P = 0.0001$, ptosis, $P = 0.0025$, tremor, $P = 0.0604$, Wetdog shake, $P = 0.0135$, weight loss, $P = 0.1332$). Higher amount of diarrhea was observed in morphine-treated groups due to spontaneous morphine withdrawal. $^{*}P < 0.05$, $^{**}P < 0.01$ vs Mor. ANOVA, analysis of variance; Mor = moprhine; NLX = naloxone.

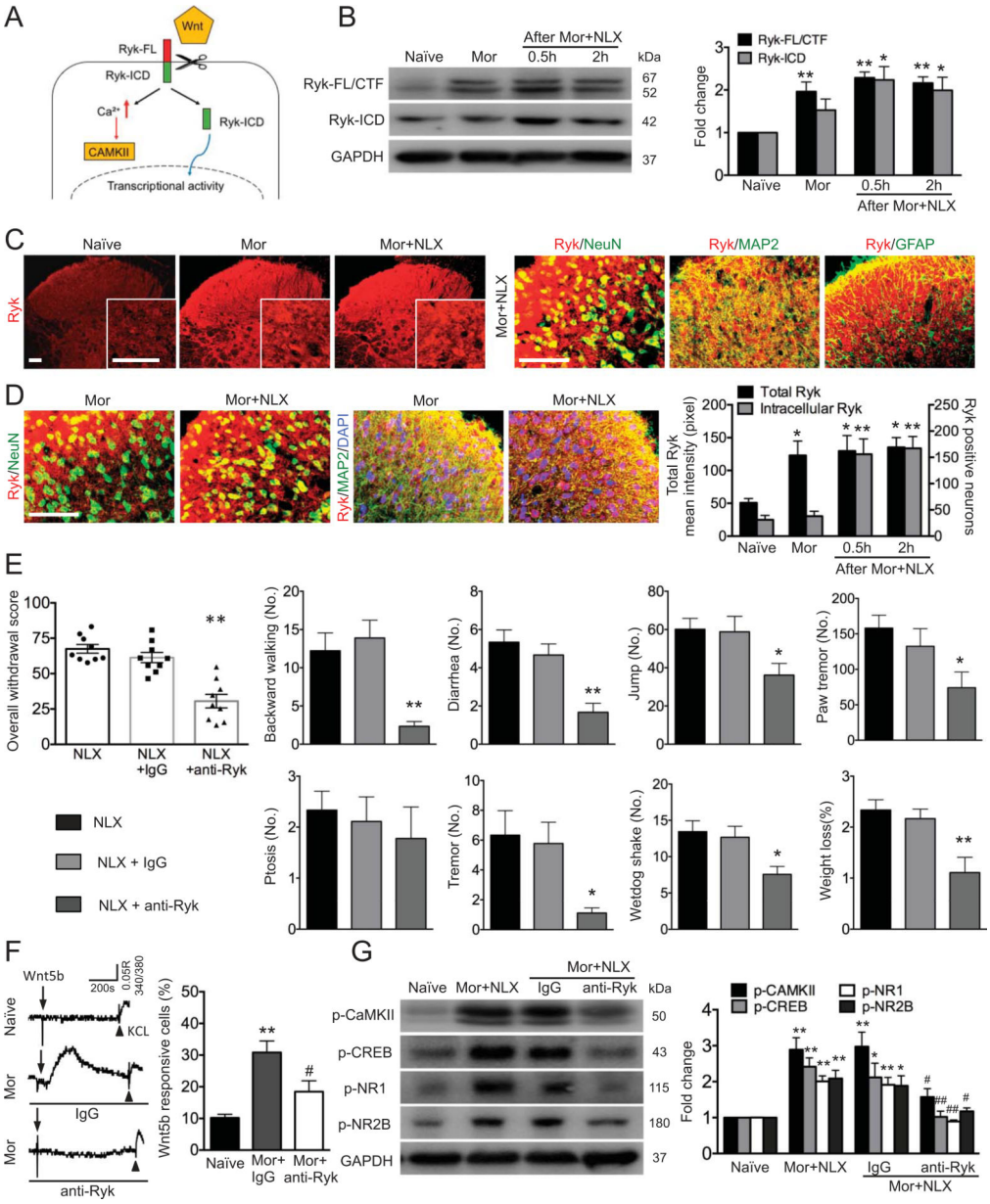

Figure 4.

Ryk receptor activation after morphine exposure and naloxone-precipitated withdrawal. (A) Schematic representation of Wnt-Ryk signaling and its downstream activation of Ca^{2+} and Ryk-ICD pathways. (B) Western blot showing expression of Ryk-FL/CTF and Ryk-ICD. Left, representative bands. Right, data summary. Ryk-FL/CTF, one-way ANOVA, $P =$ 0.0002. Bonferroni's multiple comparisons vs naive: Mor, $P > 0.0022$, after NLX, 0.5 hours, $P < 0.0002$, 2 hours, $P < 0.0005$. Ryk-ICD, one-way ANOVA, $P = 0.0233$. Bonferroni's multiple comparisons vs naive: Mor, $P > 0.4251$, after NLX, 0.5 hours, $P = 0.0149$, 2 hours, $P = 0.0345$). $^{*}P < 0.05$, $^{**}P < 0.01$ vs naive. The upper band inRyk-FL/CTF is full-length Ryk receptor (FL), while the lower band is the C terminal fragment of Ryk receptor (CTF). (C) Immunofluorescence showing expression of Ryk (red) in the DH (left) and its cellular colocalization with neuronal soma (NeuN) and dendrites (MAP2) and astrocytes (GFAP)

(right). (D) Immunofluorescence showing the cellular internalization of Ryk receptors. Neuronal soma was marked with NeuN or DAPI. Dendrite was marked with MAP2. Histogram showing the mean intensity of Ryk receptors immunofluorescent activity, (one-way ANOVA, $P = 0.0002$. Bonferroni's multiple comparisons vs naive: Mor, $P > 0.0022$, after NLX, 0.5 hours, $P < 0.0002$, 2 hours, $P < 0.0005$) (Y axis, left) and number of Ryk-positive neurons (one-way ANOVA, $P < 0.0001$. Bonferroni's multiple comparisons vs naive: Mor, $P > 0.99$, after NLX, 0.5 hours, $P = 0.001$, 2 hours, $P = 0.0004$) (Y axis, right). $^{*}P < 0.05$, $^{**}P < 0.01$ vs naive. Original magnification in and Cand D: ×800; scale bar = 50 μm. (E) Intrathecal injection of anti-Ryk (2 μg in 5 μL) suppresses the overall withdrawal scores and individual behavioral signs after naloxone-precipitated withdrawal. One-way ANOVA, $P < 0.0001$. Bonferroni's multiple comparisons vs NLX: IgG, $P = 0.5476$, after anti-Ryk, $P < 0.0001$) $^{**}P < 0.01$ vs NLX group. Individual signs, Bonferroni's multiple comparisons, NLX + anti-Ryk vs NLX, backward walking, $P = 0.0028$, diarrhea, $P = 0.0003$, jump, $P = 0.0375$, paw tremor, $P = 0.0242$, ptosis, $P = 0.8832$, tremor, $P = 0.0158$, Wetdog shake, $P = 0.0122$, weight loss, $P = 0.0024$). (F) Bath application of anti-Ryk (4 μg/mL) reduced Wnt5b (20 mM)-induced calcium transient in the primary cultured DH neurons with prolonged in vivo morphine exposure. Number of neurons: naïve = 49; Mor = 33; (Mor + anti-Ryk) = 51 in each group from 3 animals (one-way ANOVA, $P < 0.0001$. Dunnett's multiple comparisons vs Mor + IgG, naive, $P = 0.0047$, Mor + anti-Ryk, $P = 0.0445$). $^{**}P < 0.01$ vs naive, $\#P < 0.05$ vs Mor + IgG. (G) Intrathecal administration of anti-Ryk (2 μg in 5 μL) inhibits naloxone-precipitated withdrawal-induced increased phosphorylation of CaMKII (one-way ANOVA, $P = 0.0003$.Bonferroni's multiple comparisons: naïve vs Mor + NLX, $P = 0.0008$, NLX + Mor vs IgG, $P > 0.99$, vs anti-Ryk, $P = 0.0153$), CREB (one-way ANOVA, $P = 0.001$. Bonferroni's multiple comparisons: naive vs Mor + NLX, $P = 0.0026$, NLX + Mor vs IgG, $P > 0.99$, vs anti-Ryk, $P = 0.0029$), NR1 (One-way ANOVA, $P < 0.0001$. Bonferroni's multiple comparisons: naïve vs Mor + NLX, $P = 0.0002$, NLX + Mor vs IgG, $P > 0.99$, vs anti-Ryk, $P < 0.0001$), and NR2B (One-way ANOVA, $P = 0.0033$. Bonferroni's multiple comparisons: naive vs Mor + NLX, $P = 0.0043$, NLX + Mor vs IgG, $P > 0.99$, vs anti-Ryk, $P = 0.0143$) in the spinal cord. The upper band in p-CamKII is p-CamKII-β (Thr287), while the lower band is p-CamKII-α (Thr286). Tissues were collected 30 minutes after naloxone injection (n = 5 animals in each group). Left, representative bands. Right, data summary (mean ± SEM). $^{*}P < 0.05$, $^{**}P < 0.01$ vs naïve; $\#P < 0.05$, $\#\#P < 0.01$ vs Mor + NLX. Number of animals: 4, 5, and 9 in B, D, and E, respectively. Mor = morphine; NLX = naloxone.

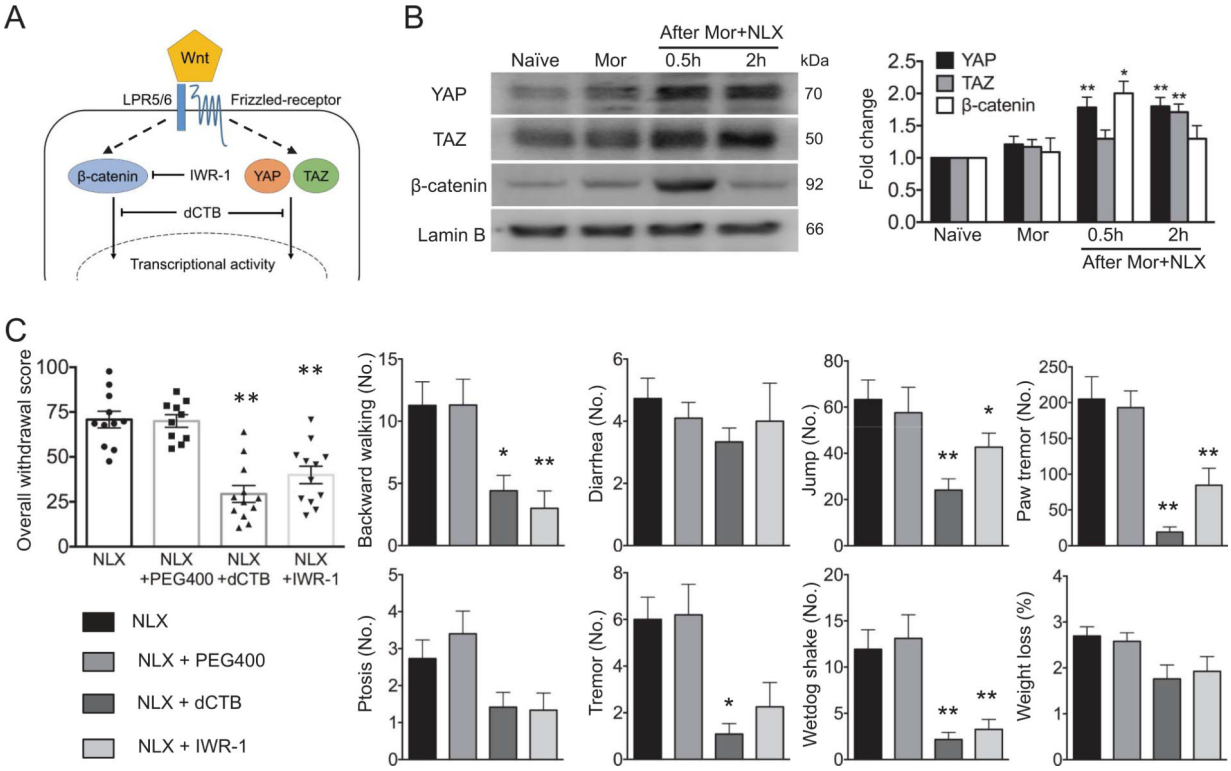

Figure 5.

Activation of the transcriptional factors YAP, TAZ, and β-catenin contributes to the development of naloxone-precipitated morphine withdrawal. (A) Schematic presentation showing canonical Wnt-β-catenin and alternative Wnt-YAP/TAZ signaling pathways and the pharmacological targets of the reagents IWR-1 and dCTB. (B) Western blot showing nuclear expression of YAP/TAZ/β-catenin. Left, representative bands. Right, data summary (mean ± SEM). Five animals in each group. YAP, One-way ANOVA, $P = 0.0004$. Bonferroni's multiple comparisons vs naive: Mor, $P = 0.7513$, after NLX 0.5 hours, $P = 0.0012$, 2 hours, $P = 0.0009$. TAZ: One-way ANOVA, $P = 0.0018$. Bonferroni's multiple comparisons vs naive: Mor, $P = 0.8354$, After NLX 0.5 hours, $P = 0.2025$, 2 hours, $P = 0.0009$, β-catenin: One-way ANOVA, $P = 0.0038$. Bonferroni's multiple comparisons vs naive: Mor, $P > 0.99$, after NLX 0.5 hours, $P = 0.0028$, 2 hours, $P = 0.7397$). $^{*}P < 0.05$, $^{**}P < 0.01$ vs naive. (C) Intrathecal administration of dCTB (200 μg in 5 μL) and IWR-1 (5 μg), respectively, significantly suppressed the naloxone-precipitated withdrawal. Nine animals in each group. One-way ANOVA, $P < 0.0001$. Bonferroni's multiple comparisons vs NLX: PEG400, $P = 0.5476$, after dCTB, $P < 0.0001$, IWR-1, $P = 0.0001$). Individual signs (Bonferroni's multiple comparisons, NLX + dCTB/IWR-1 vs NLX, backward walking, $P = 0.0143/0.0025$, diarrhea, $P = 0.6624/0.99$, jump, $P = 0.0020/0.1808$, paw tremor, $P = 0.0001/0.0015$, ptosis, $P = 0.1941/0.1502$, tremor, $P = 0.0021/0.0238$, Wetdog shake, $P = 0.0005/0.0021$, weight loss, $P = 0.06/0.1118$). $^{*}P < 0.05$, $^{**}P < 0.01$ vs NLX. ANOVA, analysis of variance; Mor = morphine; NLX = naloxone.

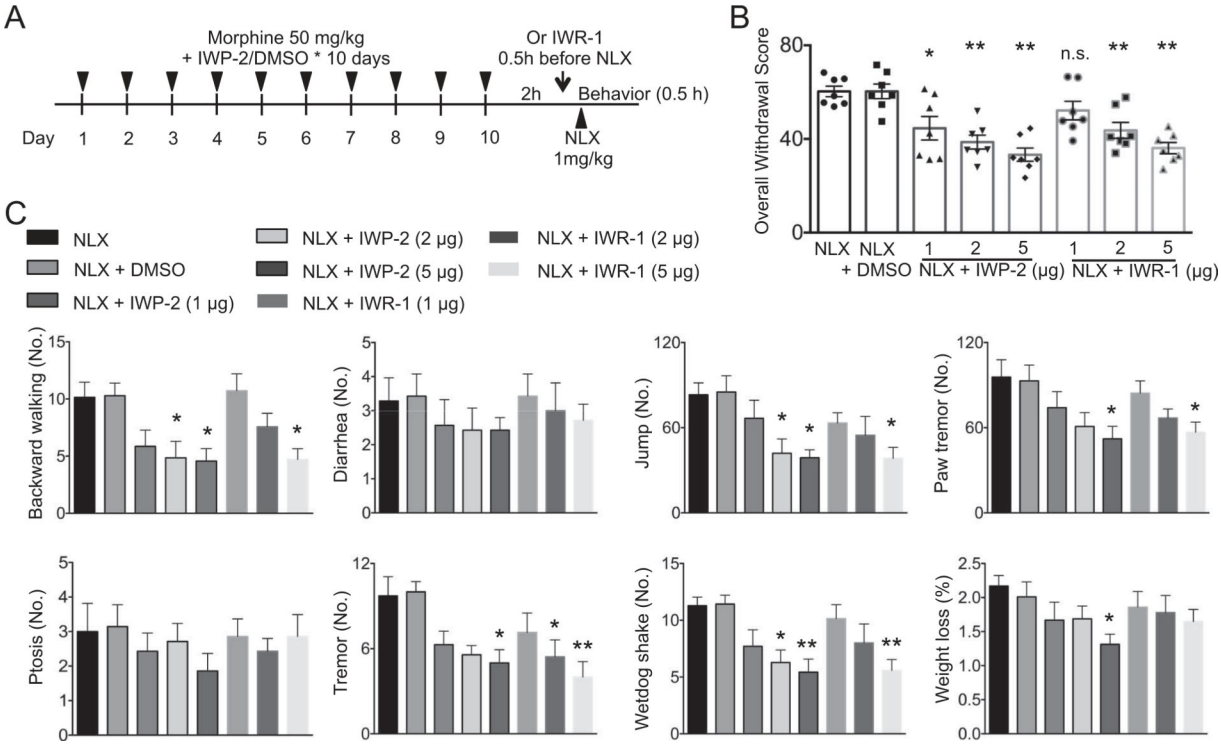

Figure 6.

Inhibition of Wnt signaling suppresses NLX-induced withdrawal behaviors after chronic morphine administration at fixed dose. (A) Schematic of experimental design, morphine was given at a fixed dose (intraperitoneally, 50 mg/kg/day) for 10 consecutive days before naloxone treatment. (B and C) Intrathecal administration of morphine with Wnt synthesis inhibitor IWP-2 or with canonical pathway inhibitor IWR-1, both in 1, 2, and 5 μg, produced dose-related suppression on the naloxone-induced withdrawal overall score (B) and individual behaviors (C). Seven animals in each group. One-way ANOVA, $P < 0.0001$. Bonferroni's multiple comparisons vs NLX: IWP-2, 1 μg, $P = 0.121$, 2 μg, $P = 0.0002$, 5 μg, $P < 0.0001$. IWR-1, 1 μg, $P = 0.637$, 2 μg, $P = 0.0068$, 5 μg, $P < 0.0001$). $*P < 0.05$, $**P < 0.01$ vs NLX. Individual behavioral signs, Bonferroni's multiple comparisons vs NLX, $*P < 0.05$, $**P < 0.01$ vs NLX.

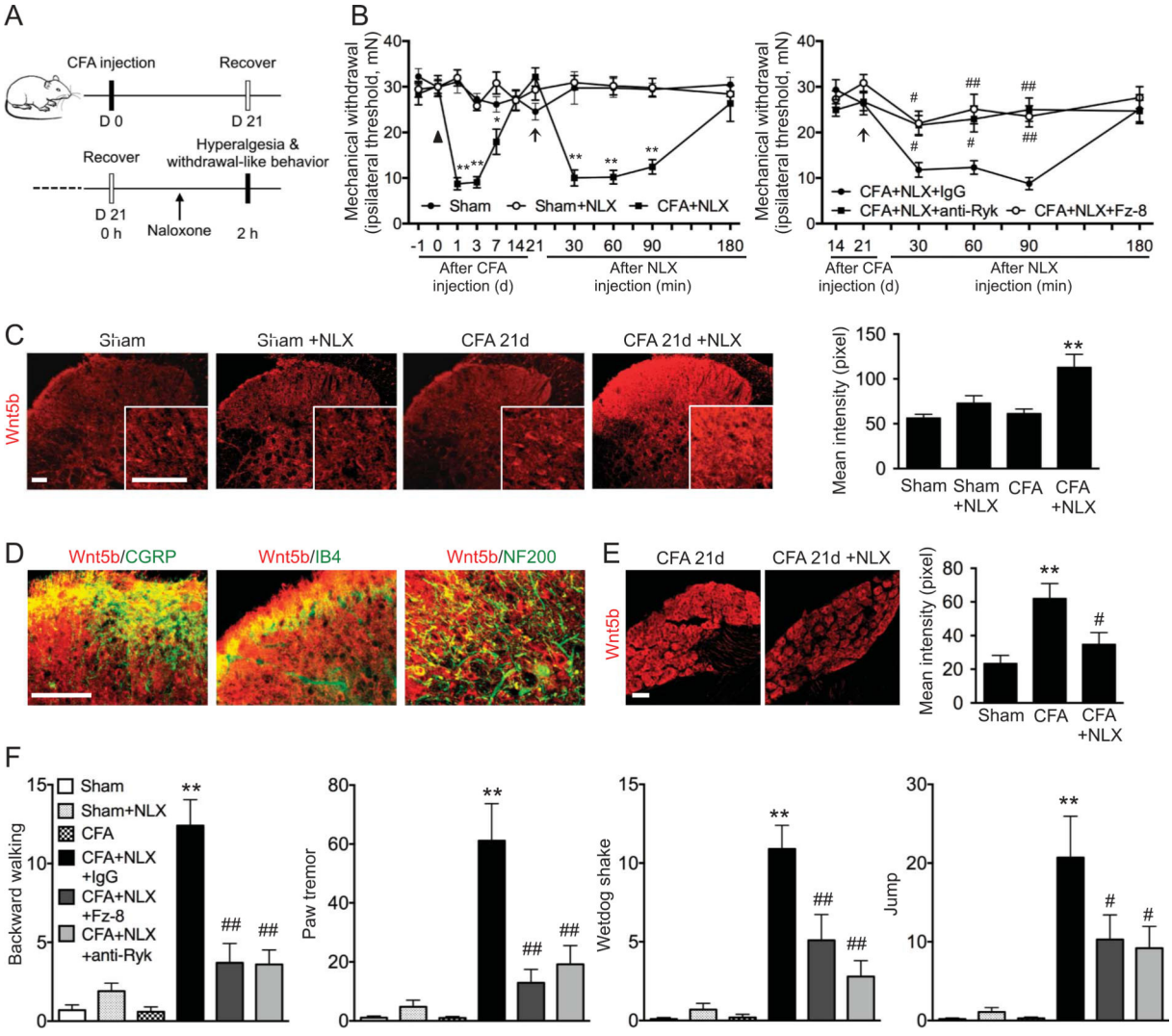

Figure 7.

WNT signaling contributes to the withdrawal from opioid receptor activation following CFA-induced chronic inflammation in mice. (A) Schematic representation showing the experimental procedure of the NLX-induced mechanical allodynia testing. (B) Intrathecal administration (in 5 μL) of anti-Ryk (2 μg) and Fz-8/Fc (2 μg), respectively, suppressed the mechanical allodynia. Eight animals were included in each group. Two-way ANOVA, Bonferroni's multiple comparisons Sham vs CFA + NLX, 1, 3 day, $P < 0.0001$, 7 day, $P = 0.0140$, after NLX, 30, 60, 90 minutes, $P < 0.0001$, 180 minutes, $P = 0.4597$. After anti-Ryk/Fz-8, two-way ANOVA, Bonferroni's multiple comparisons vs CFA + NLX + IgG, 30minutes, $P = 0.0335/0.0495$, 60minutes, $P = 0.0020/0.0223$, 90minutes, $P = 0.0002/0.0001$, 180 minutes, $P > 0.99$). The solid triangle indicates CFA injection, and the arrow indicates drug injection. $*P < 0.05$, $**P < 0.01$ vs Sham; $\#P < 0.05$, $\#\#P < 0.01$ vs CFA + NLX + IgG. (C–E) Immunofluorescence showing expression of Wnt5b (red) and its colocalization with the CGRP-, IB4-, and NF200-positive afferents (C–D) in the DH as well as Wnt5b expression in the DRG (E) 21 days after CFA injection. Five animals were included in each group. In C, one-way ANOVA, $P = 0.0235$. Bonferroni's multiple

comparisons vs Sham: Sham + NLX, $P = 0.9272$, CFA, $P > 0.99$, CFA + NLX, $P = 0.0178$. In E, CFA vs Sham: Sham, $P = 0.0047$, CFA vs CFA + NLX, $P = 0.0380$). Original magnification: ×200, scale bar = 50 μm (C and E); ×800, scale bar = 50 μm (D). (F) Effects of intrathecal anti-Ryk and Fz-8/Fc on naloxone-induced withdrawal-like behaviors on the 21 days after CFA injection. The anti-Ryk or FZ-8/Fc was given 30 minutes before naloxone injection. Ten animals were included in each group. Backward walking, one-way ANOVA, $P < 0.0001$. Bonferroni's multiple comparisons CFA + NLX + IgG vs Sham, $P < 0.0001$, Fz-8/Fc vs IgG, $P < 0.0001$, anti-Ryk vs IgG, $P < 0.0001$, paw tremor: one-way ANOVA, $P < 0.0001$. Bonferroni's multiple comparisons CFA + NLX + IgG vs Sham, $P < 0.0001$, Fz-8/Fc vs IgG, $P < 0.0001$, anti-Ryk vs IgG, $P < 0.0001$, Wetdog shake: One-way ANOVA, $P < 0.0001$. Bonferroni's multiple comparisons CFA + NLX + IgG vs Sham, $P < 0.0001$, Fz-8/Fc vs IgG, $P = 0.0005$, anti-Ryk vs IgG, $P < 0.0001$, jump: one-way ANOVA, $P < 0.0001$. Bonferroni's multiple comparisons CFA + NLX + IgG vs Sham, $P < 0.0001$, Fz-8/Fc vs IgG, $P = 0.0292$, anti-Ryk vs IgG, $P = 0.0135$). $^{**}P < 0.01$ vs Sham; $^{\#}P < 0.05$, $^{\#\#}P < 0.01$ vs CFA + NLX + IgG. ANOVA, analysis of variance; CFA, complete Freund's adjuvant; NLX = naloxone.